



An air-cooled proton exchange membrane fuel cell with combined oxidant and coolant flow

Jinfeng Wu^a, Stefano Galli^b, Ivano Lagana^b, Afonso Pozio^b, Giulia Monteleone^b, Xiao Zi Yuan^a, Jonathan Martin^a, Haijiang Wang^{a,*}

^a Institute for Fuel Cell Innovation, National Research Council Canada, Vancouver, BC, Canada V6T 1W5

^b ENEA, C.R. Casaccia, S.P. 55, Technologie Energetiche Avanzate, Via Anguillarese 301, S. Maria di Galeria, Rome 00060, Italy

ARTICLE INFO

Article history:

Received 15 October 2008

Received in revised form

13 November 2008

Accepted 14 November 2008

Available online 28 November 2008

Keywords:

Proton exchange membrane fuel cells

Air-cooled

Combined flow

Open cathode design

Membrane electrode assembly

Stack

ABSTRACT

Combining the oxidant and coolant flow in an air-cooled proton exchange membrane fuel cell can significantly simplify the fuel cell design. In this paper, an air-cooled PEM fuel cell stack with an open cathode flow field, which supplied the oxidant and removed the heat produced in the fuel cell, was fabricated and tested. The influence of different operating parameters on cell voltage performance and the overall cell ohmic resistance, such as cell temperature and airflow rate, was investigated. The cell temperature and the temperature difference between the cell and the hydrogen humidifier were shown to serve important roles in reducing the fuel cell ohmic resistance. The test results also showed a noteworthy temperature gradient between each cell of a 5-cell stack. A hydrophilic treatment of the cathode flow field channels was demonstrated to be an effective way to mitigate water management issues caused at elevated operating temperatures.

Crown Copyright © 2008 Published by Elsevier B.V. All rights reserved.

1. Introduction

To increase the electrochemical reaction rate and promote fuel cell output efficiency, pressurized reactants and liquid cooling are vastly preferable. According to the available literature, the ideal operational conditions for proton exchange membrane (PEM) fuel cells include a pressure of about 3 atm and a temperature of about 80 °C [1]. However, these operating conditions conversely lead to auxiliary requirements, such as a gas cylinder and/or gas compressor and a liquid cooling pump, thus increasing parasitic losses from the fuel cell system and ultimately weakening the merits of the system over other power sources. On the other hand, the demand for high-voltage fuel cell output drives the stacking of single cells. The most common stacking format currently in use is placing the anode of one cell adjacent to the cathode of another and connecting them electrically in series via bipolar plates [2].

In order to improve gross efficiency and simplify fuel cell design, work has been undertaken in the past few decades to employ different configurations, such as air-breathing and air-cooled PEM fuel cells and stacks. An air-breathing fuel cell does not employ a compressed flow of oxidant or air past the cathodes, but instead utilizes ambient air and relies on natural convection in the surrounding

environment. The design output power of this kind of PEM fuel cell is normally less than 1 W, due to its passive, self-breathing operation, making it suitable as a replacement for batteries in a wide range of portable electronic devices. Two types of air-breathing fuel cell design, i.e., tubular [3] and planar [4–6], have been the primary foci of investigation to date. Green et al. studied the effect of different current collector materials and cathode hole sizes on a tubular air-breathing fuel cell [3]. Schmitz et al. [4] looked at the impacts of the size of the cathode opening and the wetting properties of the diffusion layer on the performance of planar air-breathing PEM fuel cells. Nopenen et al. [5] and Hottinen et al. [6] individually measured steady-state and transient current density distribution in free-breathing PEM fuel cells by adopting the sub-cell approach. However, one issue inherent to both tubular and planar design is the significantly complicated configuration of air-breathing fuel cell stack designs. The series connection of a fuel cell stack is achieved by electrically connecting an anode with the cathode of the adjacent cell in a “flip-flop” configuration, in which the individual fuel cells are arranged along a common axis or plane [7].

Though both air-breathing and air-cooled PEM fuel cell modules can currently be purchased commercially [8,9], relatively little attention has been devoted to the systematic development of air-cooled fuel cell designs. An open cathode design is usually employed for air-cooled PEM fuel cells and forced air is supplied to the cathode using fans. Additional functions of the fans can include cooling the cell and stack, and accelerating the evaporation

* Corresponding author. Tel.: +1 604 221 3038; fax: +1 604 221 3001.

E-mail address: haijiang.wang@nrc-cnrc.gc.ca (H. Wang).

of the byproduct water from the electrochemical reaction to avoid flooding. Compared with an air-breathing PEM fuel cell stack, an air-cooled fuel cell and stack has the advantages of easy operation and simple stacking. The conventional stacking design can be used, due to the integration of the reactant gas supply and the cooling system. Recently, the Ballard Mk1020 ACS fuel cell stack with an open cathode design and a wide power output scale from 300 W to 4 kW was reported [10]; the influences of ambient temperature, ambient humidity, altitude, and air contamination on the performance of the Mk1020 ACS stack were studied. However, detailed information about the flow field configurations has not been released.

As presented in this paper, a single air-cooled PEM fuel cell with an open cathode flow field was designed and fabricated using desktop milling [11] and membrane electrode gasket assembly (MEGA) technologies [12]. The influences of the different operational conditions, such as air fan voltage and cell temperature, on the performance of an air-cooled PEM fuel cell were evaluated. Based on the results of single-cell tests, a small stack with five cells was set up and preliminary testing results of this stack were obtained.

2. Experiments

2.1. Membrane electrode gasket assembly

Electrodes were prepared by a spray technique using carbon-supported (30% Pt/C and 30% Pt–Ru/C) catalysts (E-TEK Inc.), carbon powders (Vulcan XC72, Cabot), carbon paper substrates (TGP-H-090, Toray), polytetrafluoroethylene (PTFE) dispersions (35 wt% PTFE aqueous dispersion, Hostaflon 5033, Hoechst, Nafion® solutions (5 wt% Nafion® 1100 EW solution, Solution Technology), and glycerol. The Pt–Ru catalyst loading at the anode side and the Pt loading at the cathode side were both kept at 0.54 mg cm^{-2} . Nafion® loadings on the anode and cathode were controlled at 0.9 and 1.35 mg cm^{-2} , respectively. The membrane electrode assembly (MEA) was fabricated by hot pressing the electrodes onto the Nafion® 115 membrane from both sides under a pressure of $50\text{--}100 \text{ kg cm}^{-2}$ at 130°C for 1–5 min. All MEAs utilized in this paper had the same active areas of 50 cm^2 . Finally, MEGA technology was employed to produce a well-defined shape compatible with the cell hardware [12].

2.2. Graphite flow field plates

The anode and cathode plates were made from commercially available graphite material BMA5 from SGL Carbon Group (Germany), which is hydrophobic with a low-electrical resistivity of $100 \mu\Omega \text{ m}$ (in plane). Different anode and cathode flow field configurations were manufactured by using a desktop compact computer numerical control 3D mini-milling machine with which machining accuracy was controlled to within 0.01 mm [11]. Fig. 1(a) shows the structure of the open flow field used at the cathode, which consisted of 12 parallel channels with straight channels in the middle and bends at both ends. Each channel was 3 mm in width and 1.5 mm in depth with a land width of 2 mm. For the anode plate, a 3-channel serpentine flow field (1 mm in channel width and 1 mm in channel depth) was designed, as shown in Fig. 1(b).

2.3. System setup

In addition to anode and cathode flow field plates, the fuel cell hardware consisted of two flat graphite plates and two gold-coated copper plates as current collectors and end plates, respectively. The cell temperature was controlled with heating rods placed inside the two copper plates. Hydrogen was fully humidified at a constant temperature of 55°C prior to its delivery to the fuel cell and its stoichiometry was controlled at 2. Ambient air was supplied directly by utilizing a DC air fan by utilizing a DC air fan [13] (Papst 414, 24

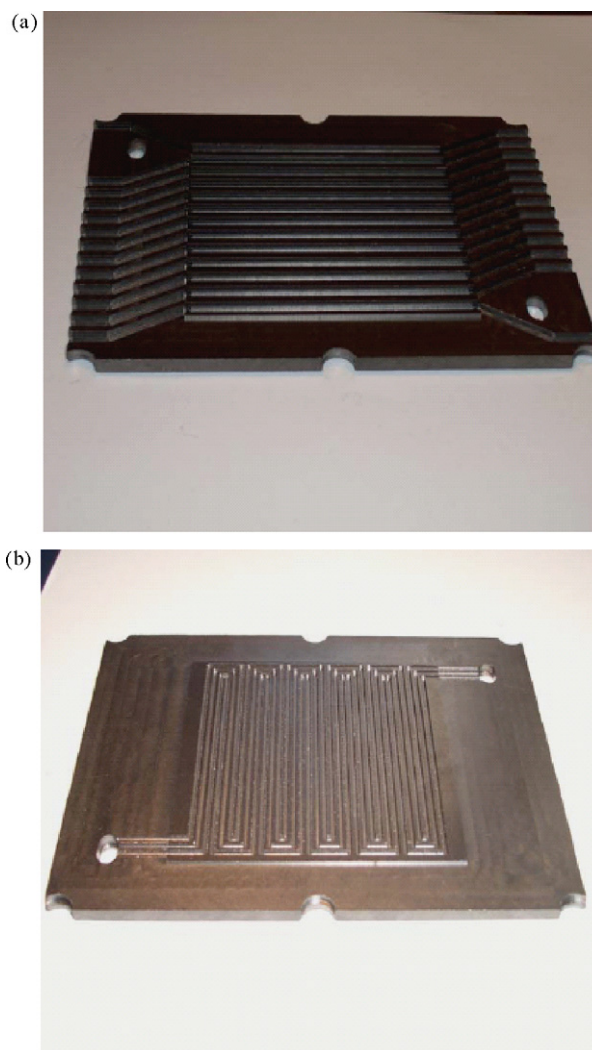


Fig. 1. The graphite flow field plates used in an air-cooled fuel cell with an open cathode design: (a) cathode plate with open channels; (b) anode plate with three serpentine channels.

VDC, Series 400, Cool Power Solutions) without humidification. In order to ensure uniform air distribution, the fan was inserted into a plenum with a slot that had the same dimensions as the underside of the fuel cell, as shown in Fig. 2. In this study, the cell and stack were all operated in a vertical position, the dry air flowed from the bottom up, and its flow rate in the cathode flow field was adjusted by changing the fan voltage. As a result of the open cathode design, it is relatively difficult to measure the in situ air flow rate or pressure drop in the channels. Therefore, air fan voltage, rather than air flow rate and pressure drop, is treated as one of the operational parameters in this paper. The experiments were performed on a commercial fuel cell test station (model 890, Globe Tech Inc.), which was equipped with mass flow controllers, bubblers for reactant humidification, and a programmable electric load. The current pulse transient technique was utilized to measure the overall ohmic resistance of the fuel cell [14].

3. Results and discussion

3.1. Air-cooled single PEM fuel cell test

Fig. 3 shows the single-cell polarization curve with the open cathode design when fan voltage and cell temperature were

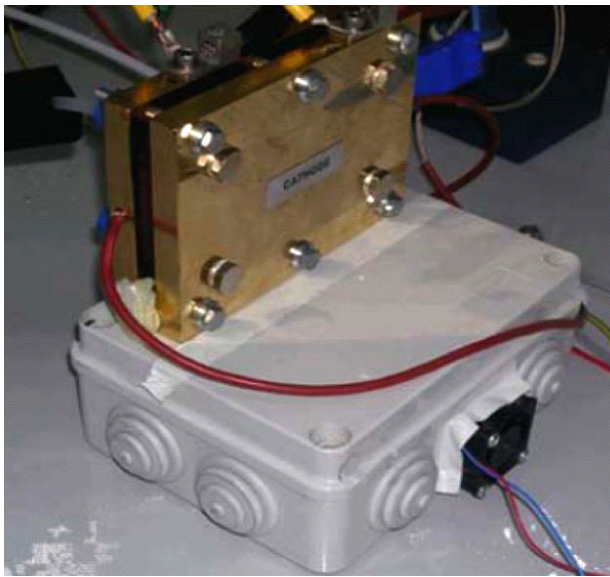


Fig. 2. Air-cooled single PEM fuel cell setup with air fan and plenum.

controlled at 7.5 V and 40 °C, respectively. For comparison, the performance of the same MEGA under conventional conditions – i.e., fully humidified air and hydrogen at 40 °C fed to the cell under pressurized conditions of 2.0 bara and air/hydrogen stoichiometry of 3/2 – is also presented. For the conventional pressurized single cell, the maximum power density is 247 mW cm⁻² at a cell potential of 0.5 V, while the cell with an open cathode design and without external air humidification can reach 87 mW cm⁻² at a cell potential of 0.4 V, which is approximately one-third of the maximum power density under conventional pressurized conditions. One reason for the relatively low performance of the air-cooled single cell with an open cathode design is the low-operating air pressure provided by the air fan, which is only slightly above the atmosphere pressure and much lower than that under conventional pressurized conditions. The lower operating air pressure results in a decreased oxygen partial pressure, which reduces the reaction rates and raises the activation overpotential. Furthermore, decreased operating pressure is disadvantageous for enhancing the diffusion rates of the reactants to the active sites, resulting in a significant increase in cell concentration overpotential. Another reason for this behavior is that besides the open cathode design, the air-cooled PEM fuel cell

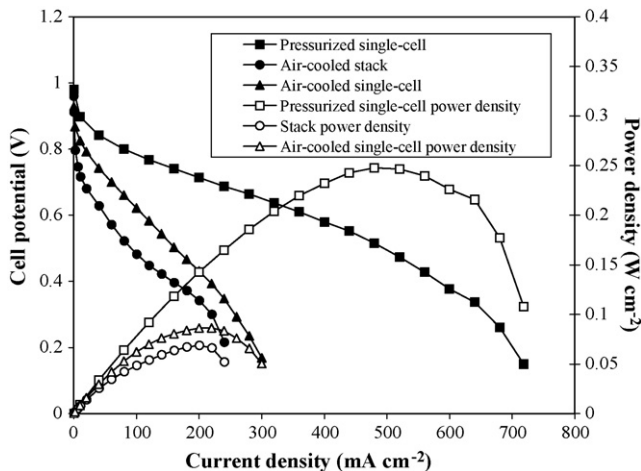


Fig. 3. Polarization curve and power density curve for the conventional pressurized fuel cell, air-cooled single fuel cell, and air-cooled fuel cell stack, respectively.

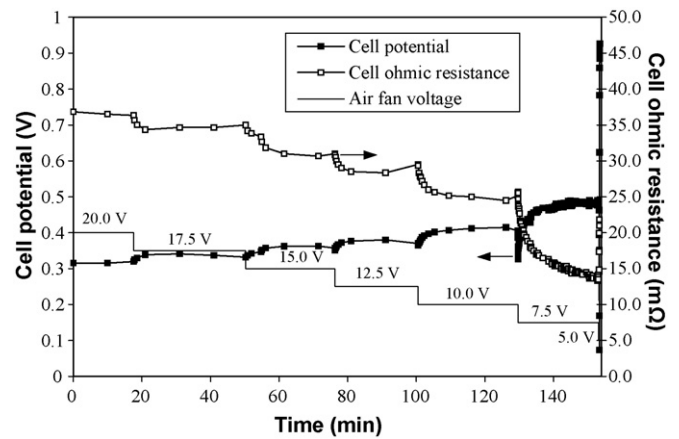


Fig. 4. Impact of air fan voltage step decrease on the cell potential and overall ohmic resistance under a fixed load of 120 mA cm⁻².

is operated without external air humidification. Therefore, water management becomes a major challenge. For example, in the case of high-air flow rate and/or low-current density, the amount of water removed from the cell may be higher than the amount of water generated, resulting in membrane drying and inferior performance.

Single-cell voltage and relative cell ohmic resistance in response to the stepwise decrease of air fan voltage is shown in Fig. 4. During the measurement procedure, the fuel cell was operated at a fixed current density of 120 mA cm⁻² and the cell temperature was maintained at 50 °C. Considering that the hydrogen humidification temperature was 55 °C, the hydrogen was fully humidified prior to its introduction into the cell. Clearly, the fuel cell performance and ohmic resistance show opposite responses to the decrease in air fan voltage, i.e., the cell performance increases and the ohmic resistance decreases with decreasing fan voltage.

When the fan is controlled at a voltage of 20.0 V, the pressure drop in the cathode flow channels is comparatively high. It is believed that at the cathode side, most of the water generated by the electrochemical reaction and forced from the anode side is removed from the cell by the forced air. Therefore, there is insufficient water to keep the MEA well humidified, resulting in a relatively high-cell ohmic resistance of 36.8 mΩ and a concurrently low-cell potential of 0.315 V.

With a decrease of the air fan voltage from 17.5 to 10.0 V, the air flow rate and the associated pressure drop in the cathode channels both decrease and, as a result, more water is preserved in the cathode side. This can mitigate membrane dryness and increase the hydration of the ionomer in the catalyst layer. The cell ohmic resistance drops from 35 to 25 mΩ, and meanwhile the cell performance continuously increases from 0.34 to 0.415 V. However, it is observed that with the decrease in air flow rate, cell voltage instability becomes apparent during the initial stage of the fan voltage change. Moreover, this voltage oscillation effect becomes more pronounced when the fan voltage is reduced from 10.0 to 7.5 V. Cell voltage instability during both the initial stage of fan voltage change and the oscillation at fan voltages below 10.0 V can be explained as an indication of excess liquid water in certain areas of the electrode and/or in the open flow channel(s). When the fan voltage is as low as 5.0 V, the cell voltage drops below the minimum (0.02 V) and the system shuts down automatically.

Residual water resulting from insufficient gas flow and decreased pressure drop will block oxygen from reaching the cathode. This liquid water accumulation may cause critical water management issues in the cell, such as maldistribution of the reactant gas in the flow channels, flooding and inactivity of the catalyst layer, and/or limited oxygen permeability through the gas

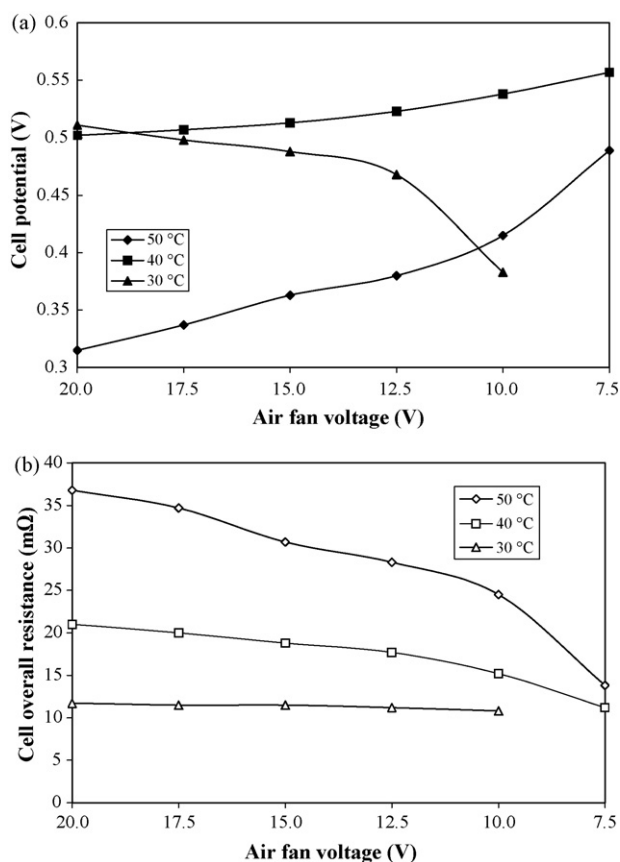


Fig. 5. Impact of cell operating temperature on the cell potential (a) and overall ohmic resistance (b) under a fixed load of 120 mA cm^{-2} .

diffusion layer to the catalytic sites. On the other hand, poor cell water management in the open cathode design under low-fan voltage can also lead to erratic performance, loss of efficiency, and even operating failure, as shown in Fig. 4.

The influence, under different cell temperatures, of air fan voltage on both cell potential and overall ohmic resistance is shown in Fig. 5(a) and (b), respectively. Clearly, among the testing cell temperatures of 50, 40, and 30 °C, the best performance is achieved when the cell is operated at 40 °C. In the case of a cell temperature of 40 °C and the hydrogen humidified at 55 °C, the hydrogen is relatively over-humidified before being fed to the anode side, due to the elevated temperature difference between the cell and the humidifier, which eventually promotes water transfer from the anode to the cathode. It can be observed that the cell perform better within almost the entire range of air fan voltages, in spite of the lower kinetics as compared with the cell at 50 °C. The better performance may also be attributed to decreased water loss due to evaporation at 40 °C, which increases the water content in the MEA. Thus, in the case of operation at 40 °C, the larger temperature difference between the humidifier and the cell and the elevated cell operating temperature all account for the improved cell performance, due to improved water balance in the air-cooled fuel cell with an open cathode design. Also, compared with the case when the cell is operated at 50 °C, the overall cell ohmic resistance at 40 °C is always lower, indicating that the membrane and the ionomer in the catalyst layer are better hydrated. In addition, the slower drop in the cell ohmic resistance as fan voltage decreases at 40 °C, compared with at 50 °C, implies that water balance depends less on operating conditions at 40 °C. When the air fan voltage is controlled at 7.5 V, the values of the cell ohmic resistances in both cases become very close and each case reaches its highest performance within the test-

ing range, which shows that better water balance can be obtained under lower air flow rates.

A cell temperature of 30 °C was maintained in order to acquire performance information about this air-cooled fuel cell design close to room temperature. As shown in Fig. 5(a), superior performance is achieved at 30 °C when the fan is controlled at an elevated voltage of 20.0 V. Contrary to the trend that occurs when the cell is operated at elevated temperatures of 40 and 50 °C, the cell potential decreases steadily at 30 °C within a fan voltage range of 20.0 to 12.5 V, followed by an abrupt drop after the fan voltage is reduced to 10.0 V. This drop may be caused by the reduced oxygen transfer rate and/or the inactivity of certain catalytic sites. When the air fan voltage is below 10.0 V, the cell voltage oscillation increases significantly, dropping below the limiting level (0.02 V) and resulting in automatic system shutdown. The cell ohmic resistance remains at an almost constant value of $11.0 \text{ m}\Omega$ within the fan voltage range of 20.0 to 10.0 V.

3.2. Air-cooled PEM fuel cell stack test

A 5-cell stack (active area of 50 cm^2 for each cell) was designed and assembled in our lab with this new anode and cathode plate design, as shown in Fig. 6(a) and (b). Unlike in single-cell experiments, no heating device was employed during stack performance measurement.

The average cell performance is also shown in Fig. 3 for comparison with the performance when fan voltage is controlled at 10.0 V. Within the current density range, the average cell performance of the stack is a little lower than that of a single cell. This performance drop could be the result of the increased electrical resistance, uneven air distribution in the stack, and low-operating temperature. In terms of maximum power density, the 5-cell stack with an open cathode design and without a heating device can reach 69 mW cm^{-2} at a cell potential of 0.4 V, which is slightly lower than that of a single cell, 87 mW cm^{-2} . However, this result verifies the feasibility of assembling a stack with current technologies and designs, even though the stack itself is not yet optimized. It is worth noting that in Fig. 3, the performance difference between an average cell in the stack and a single cell is reduced when the current density increases beyond 120 mA cm^{-2} . This decrease in the performance difference between a single cell and the average of the stack may be due to the elevated temperature gradient and/or the uneven air distribution in the stack. Fig. 7 shows the temperature distribution of each cell in the stack when the current density is controlled at 200 mA cm^{-2} . For the cell located in the middle of the stack, the cell temperature reaches approximately 42 °C, which is 8 °C higher than in the cells at the ends, and results in better performance. In the case of a liquid cooling design, the temperature difference between each cell in a stack can be significantly reduced. However, when an air-cooled design is introduced, the remarkable temperature difference between each cell is unavoidable, and is attributable to the intrinsic poor efficiency of the air-cooled method. Based on previous experimental results with a single cell, this temperature gradient in the stack likely leads to different performance levels between the cells, and the associated critical water management issue.

3.3. Influence of cathode surface treatment on cell performance

The temperature gradient between the cells or within each cell is undoubtedly prone to becoming more pronounced with increasing cell number or size in a stack. In order to reduce the performance loss at operating temperatures higher than 50 °C, especially for cells in the middle of a stack, the surface of the cathode flow channels is treated with solubilized polymer hydrophilic material, followed by thermal treatment to polymerize the material. The rib surface of the cathode plate is not subjected to the hydrophilic treatment, to avoid increased contact resistance between the MEA and the

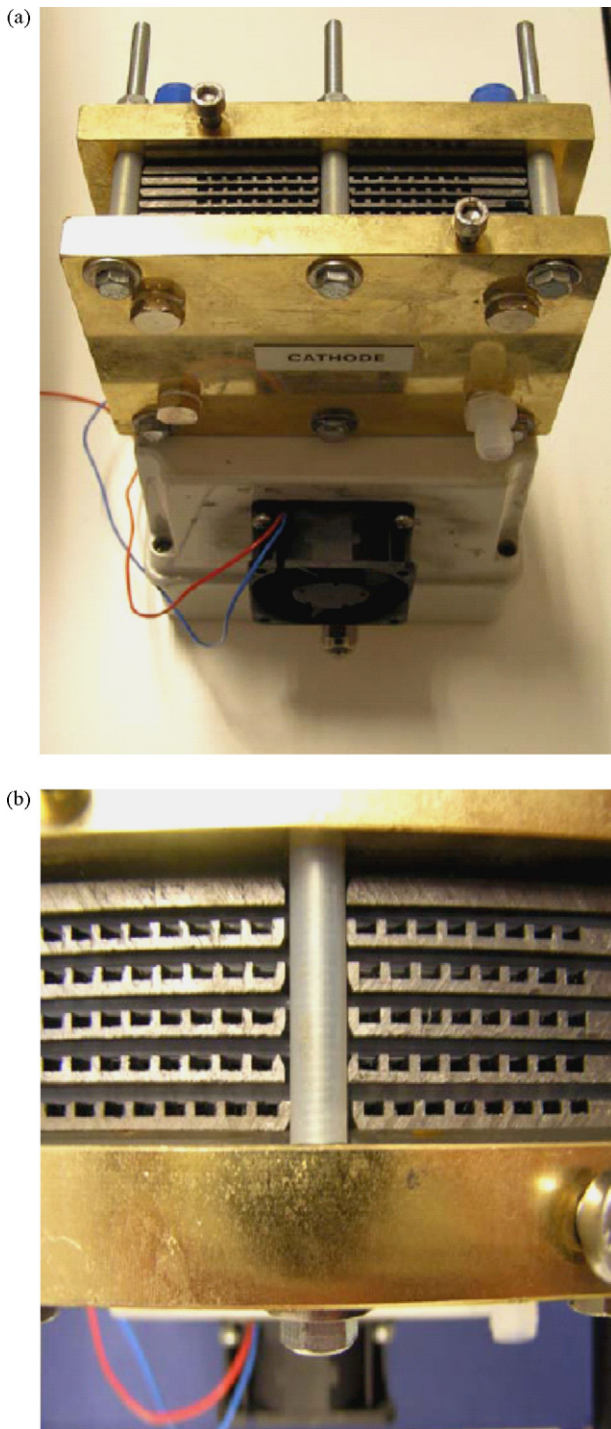


Fig. 6. Air-cooled PEM fuel cell stack setup with air fan and plenum: (a) 5-cell stack with open cathode design; (b) partial enlarged view of the stack.

cathode plates. Another MEGA with the same catalyst and Nafion® loadings was used in this experiment. Meanwhile, there was no change in the anode plate or operating conditions. The testing was carried out at a cell temperature of 40 °C and a fixed current density of 160 mA cm⁻².

Fig. 8 shows the influence that hydrophilic treatment of the cathode flow channel surface has on cell performance, as well as on the overall ohmic resistance. For both untreated hydrophobic and hydrophilic-treated cathode plates, the overall cell ohmic resistances show a similar trend, decreasing with the fan voltage. Obviously the overall resistance with the hydrophilic-treated cath-

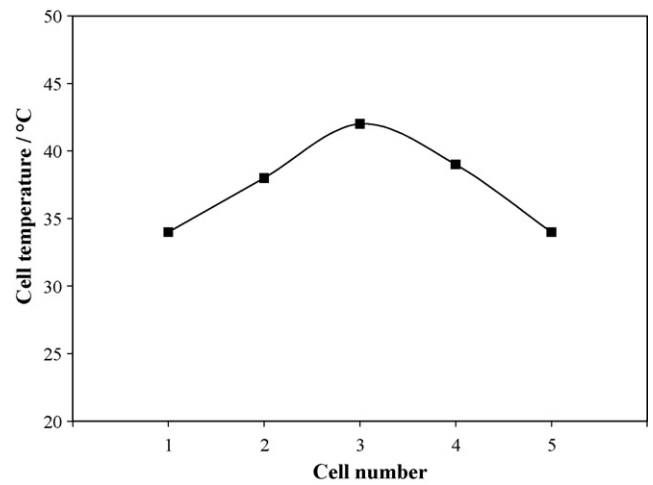


Fig. 7. Temperature distribution in the 5-cell stack under a load of 200 mA cm⁻².

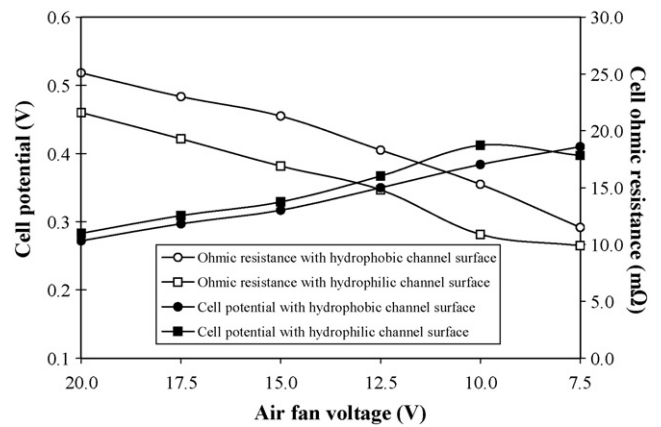


Fig. 8. Impact of hydrophilic treatment of the cathode flow channel surface on the cell potential and overall ohmic resistance under a fixed load of 160 mA cm⁻².

ode plate is significantly lower than with the hydrophobic cathode plate, within the whole range of fan voltage. As a result, when the fan voltage is controlled between 20.0 and 10.0 V, the cell performance is clearly higher with the hydrophilic cathode plate than without treatment. Maximum performance with the hydrophilic-treated cathode plate is achieved with the fan voltage at approximately 10.0 V. However, similar to the results shown in Fig. 5(a), the cell potential with the hydrophobic cathode plate steadily increases as fan voltage decreases, and reaches maximum performance at a fan voltage of 7.5 V. Thus, it can be concluded that the hydrophilic material on the cathode channel surface may have benefits in mitigating water management issues for the PEM fuel cell with an open cathode design, at relatively high-operating temperatures. This is due to the presence of the hydrophilic material, which raises the relative humidity of the reactant gas and further increases the water content in the MEA. For the cathode bipolar plates subjected to hydrophilic treatment, the overall cell-to-cell flow distribution in the stack and the uniform distribution in the flow channels of each cell are critical to ensure sufficient flow rate and pressure drop, thereby avoiding water clogging in certain flow channels.

4. Conclusions

An air-cooled single PEM fuel cell and a 5-cell stack with an open cathode design have been developed in this study. The impact of air fan voltage and cell temperature on cell performance and ohmic resistance was studied. The results showed that the tem-

perature difference between the cell and the hydrogen humidifier played an important role in reducing overall fuel cell resistance. The temperature difference between each cell in the stack with the open cathode design was found to be significantly high. In order to reduce performance loss at high-cell temperatures, an approach is proposed in which the channel surface of the cathode flow field plate is hydrophilically treated. Hydrophilic treatment of the cathode plate demonstrated improved water management when the fuel cell was operated at high temperatures.

For an air-cooled PEM fuel cell, the open cathode design plays a major part in improving cell performance. Investigating the effects that different flow field designs and cathode plate dimensions have on water management and cell performance will be the next step in our research. Further work will also focus on optimization of air-cooled stacks with open cathode designs, and the quantitative measurement, with changing fan voltage, of the air flow rate in cathode flow channels. Hydrophilic treatment will be optimized to improve water management, especially for cathode bipolar plates located in the middle of the stack. Another alternative for improving water management may be to use thinner Nafion[®] membrane instead of Nafion[®] 115 in the MEGA.

Acknowledgements

The financial support of the Casaccia Research Center (ENEA, Italy) is gratefully acknowledged. The authors also wish to thank the National Research Council of Canada (NRC)-Helmholtz and

NRC-MOST cooperative research programs for supporting the publication of this article.

References

- [1] S. Srinivasan, B. Kirby, in: S. Srinivasan (Ed.), *Fuel Cells: From Fundamentals to Applications*, Springer Science+Business Media, 2006, pp. 441–573.
- [2] S. Gottesfeld, T.A. Zawodzinski, in: R.C. Alkire, H. Gerischer, D.M. Kolb, C.W. Tobias (Eds.), *Advances in Electrochemical Science and Engineering*, vol. 5, Wiley-VCH, Weinheim, 1997, pp. 195–301.
- [3] K.J. Green, R. Sree, J.B. Lakeman, *J. New Mater. Electrochem. Syst.* 5 (2002) 1–7.
- [4] A. Schmitz, M. Tranitz, S. Eccarius, A. Weil, C. Hebling, *J. Power Sources* 154 (2006) 437–447.
- [5] M. Noponen, T. Mennola, M. Mikkola, T. Hottinen, P. Lund, *J. Power Sources* 106 (2002) 304–312.
- [6] T. Hottinen, M. Noponen, T. Mennola, O. Himanen, M. Mikkola, P. Lund, *J. Appl. Electrochem.* 33 (2003) 265–271.
- [7] M. Binder, S. Gilman, R.J. Mammone, US Patent 5,783,324 (November 5, 1996).
- [8] http://www.thehydrogencompany.com/subsite_91_products.html (accessed March 2008).
- [9] <http://www.heliocentris.com/en/fuel-cell-products/fuel-cell-systems-solutions/components-systems/fuel-cell-stacks/> (accessed March 2008).
- [10] G. Skinner, 4th Annual Inter. Fuel Cell Testing Workshop, Vancouver, BC Canada, September 12–13, 2007.
- [11] S. Galli, IEA-IPHE International PEM Fuel Cell Workshop, Mol, Belgium, June 1–3, 2005.
- [12] A. Pozio, L. Giorgi, S. Galli, M. De Francesco, R.F. Silva, R. Lo Presti, A. Danzi, *J. New Mater. Electrochem. Syst.* 6 (2003) 157–162.
- [13] <http://www.coolpowersolutions.fi/Eng/tuul.40.htm> (accessed March 2008).
- [14] A. Pozio, L. Giorgi, E. Antolini, E. Passalacqua, *Electrochim. Acta* 46 (2001) 555–561.